Heliocentric Phasing Performance of Electric Sail Spacecraft

Giovanni Mengali [1], Alessandro A. Quarta [2], Generoso Aliasi [3]

Dipartimento di Ingegneria Civile e Industriale, University of Pisa, Italy

Abstract

We investigate the heliocentric in-orbit repositioning problem of a spacecraft propelled by an Electric Solar Wind Sail. Given an initial circular parking orbit, we look for the heliocentric trajectory that minimizes the time required for the spacecraft to change its azimuthal position, along the initial orbit, of a (prescribed) phasing angle. The in-orbit repositioning problem can be solved using either a drift ahead or a drift behind maneuver and, in general, the flight times for the two cases are different for a given value of the phasing angle. However, there exists a critical azimuthal position, whose value is numerically found, which univocally establishes whether a drift ahead or behind trajectory is superior in terms of flight time it requires for the maneuver to be completed. We solve the optimization problem using an indirect approach for different values of both the spacecraft maximum propulsive acceleration and the phasing angle, and the solution is then specialized to a repositioning problem along the Earth's heliocentric orbit. Finally, we use the simulation results to obtain a first order estimate of the minimum flight times for a scientific mission towards triangular Lagrangian points of the Sun-[Earth+Moon] system.

Key words: Electric Solar Wind Sail, Heliocentric phasing orbit, Optimal trajectory, Mission towards triangular Lagrangian points

Nomenclature

a	=	maximum propulsive acceleration, $[\mathrm{mm/s^2}]$
a_c	=	spacecraft characteristic acceleration, $[\mathrm{mm/s^2}]$
$\mathcal{H}$	=	Hamiltonian function
J	=	performance index
n	=	number of revolutions
O	=	primary's center of mass
r	=	Sun-spacecraft distance, $[\mathrm{au}]$
t	=	time, $[\mathrm{days}]$
T	=	orbital period, $[\mathrm{days}]$
u	=	radial component of the spacecraft velocity, $[\mathrm{km/s}]$
v	=	circumferential component of the spacecraft velocity, $[\mathrm{km/s}]$
y	=	dimensionless parameter
α	=	cone angle, $[\mathrm{deg}]$
ΔV	=	velocity variation, $[\mathrm{km/s}]$
$\Delta\theta$	=	phasing angle, $[\mathrm{deg}]$
λ_i	=	adjoint to state i
μ	=	gravitational parameter, $[\mathrm{km^3/s^2}]$
τ	=	switching parameter

Subscripts

0	=	initial, parking orbit

[1] Professor, g.mengali@ing.unipi.it.
[2] Associate Professor, a.quarta@ing.unipi.it. **Corresponding author**.
[3] Researcher, gen.aliasi@gmail.com.

1	=	perihelion, periapse
f	=	final
max	=	maximum
$\oplus$	=	Earth
$\odot$	=	Sun

Superscripts

$\cdot$	=	time derivative
$'$	=	depending on the controls

1 Introduction

The so-called phasing maneuver (or in-orbit repositioning) for a circular orbit is a classical problem of spaceflight mechanics [1,2]. It is known that such a maneuver consists in varying the angular position of a spacecraft that initially tracks a circular orbit of given radius around a celestial body. The phasing maneuver is usually studied by assuming the application of two or more impulses [1,2], and the problem is to find the total velocity variation as a function of the required angular displacement (i.e., the phasing angle) and the total flight time. Such a maneuver often requires a significant velocity variation and a corresponding substantial amount of propellant, especially when using a chemical propulsion system.

To reduce the propellant consumption, a feasible solution is to use a propulsion system with a continuous thrust and a high specific impulse, such as a classical solar electric thruster, or even a more exotic alternative, such as a propellantless propulsion system. In the latter case the existing literature [3,4,5] already offers interesting examples in which a photonic solar sail is assumed to perform a heliocentric phasing maneuver. Within this context, the aim of this work is to study the performance of a heliocentric phasing maneuver for a spacecraft whose propulsion system is constituted by an Electric Solar Wind Sail (E-sail). The E-sail is an innovative form of spacecraft propulsion system that exploits solar wind plasma momentum by repelling positive ions by means of a number of long tethers, which are biased to a high positive voltage [6], see Fig. 1.

Using an optimal approach, it is possible to find a numerical relationship between the phasing angle, the minimum (optimal) flight time and the spacecraft characteristic acceleration, i.e. the maximum propulsive acceleration of the spacecraft at a distance from the Sun equal to one astronomical unit. In particular, this paper analyzes the performance of an E-sail-based spacecraft for a mission scenario in which the circular parking orbit approximates the Earth's heliocentric orbit, thus extending the previous results of Refs. [3,4,5] that involve a photonic solar sail-based spacecraft.

The simulation results can also be used to obtain a reasonable approximation of the flight time required to transfer a spacecraft toward the Lagrange's triangular points within the Sun-[Earth+Moon] system. Accordingly, the analysis extends the results discussed in Ref. [7] (where a single value of characteristic acceleration is considered) and provides a parametric study of the E-sail performance for this significant mission scenario. Indeed a mission to the Lagrange's triangular points would allow a nearby analysis (possibly using multiple flybys) of prospective Earth trojan asteroids to be found (hopefully) in a near future.

Currently, the only known celestial body within this special family is the 2010 TK7 asteroid [8], which is in the proximity of Lagrange's point L_4. This asteroid is however difficult to reach with a rendezvous mission due to its high orbital inclination and eccentricity. On the other hand, a mission toward Lagrange's point L_5 is useful for monitoring the solar wind composition in order to forecast the geomagnetic disturbances with 4.5 days in advance [9]. Such a mission would make it possible to increase our knowledge about the interconnections between Earth and Sun through in-situ measurements [10,11], thus extending the mission scenarios considered in the Living With a Star Program of NASA. In this context, an in depth discussion of the scientific implications obtainable with a helioseismic investigation of the solar magnetism is given in Ref. [12].

The paper is organized as follows. The next section briefly summarizes the conflicting requirements between the total velocity variation and the flight time necessary to obtain a prescribed phasing angle under the assumption of a bi-impulsive and tangential maneuver. This allows us to quantify the cost of the maneuver using a chemical thruster. Section 3 illustrates the option offered by an E-sail to fulfil a phasing maneuver, where the problem is addressed within an optimal framework by minimizing the total flight time using an indirect approach. Section 4 summarizes the simulation results obtained by varying both the reference value of the E-sail propulsive acceleration, and of the (mission) phasing angle. These results are then applied to different mission scenarios including a phasing maneuver along the Earth's heliocentric orbit, an estimate of the minimum flight times required to transfer a spacecraft from the Lagrange points L_1 to L_4 (or L_5), and a discussion about the convenience of using a drift ahead or a drift behind maneuver. Some final remarks conclude the paper.

2 Position of the problem

In a simplified mission scenario, the phasing maneuver is constituted by two impulsive velocity variations, both having the same velocity variation ΔV, and the transfer trajectory is an ellipse tangent to the circular parking orbit (of radius r_0) at its apocenter or pericenter, see Fig. 2. In particular, the maneuver is performed by applying two tangential impulses, that is, two impulses along the direction of the spacecraft orbital velocity vector.

2.1 Mathematical model

The total velocity variation ΔV can be expressed as a function of the phasing angle $\Delta\theta \in [-\pi, \pi]$ along the circular parking orbit. To that end, let $n \in \mathbb{N}^+$ be the number of revolutions covered by the spacecraft during the phasing maneuver, and introduce the dimensionless parameter

$$y \triangleq \frac{\Delta\theta}{2\,\pi\,n} \tag{1}$$

It can be verified that the corresponding value of the total velocity variation is

$$\frac{\Delta V}{v_0} = 2\left|\sqrt{\frac{2\,(1-y)^{2/3}-1}{(1-y)^{2/3}}} - 1\right| \tag{2}$$

where $v_0 = \sqrt{\mu/r_0}$ is the circular velocity along the parking orbit around the celestial body of gravitational parameter μ, whereas the total flight time Δt is

$$\frac{\Delta t}{T_0} = n - \frac{\Delta\theta}{2\,\pi} \qquad \text{with} \qquad \Delta\theta \neq 0 \tag{3}$$

where T_0 is the orbital period of the parking orbit.

The case $\Delta\theta > 0$ refers to a spacecraft that drifts ahead (case A) a virtual point, along the circular orbit, which coincides with the vehicle's position at the beginning of the maneuver, see Fig. 2(a). On the other hand, the case $\Delta\theta < 0$ corresponds to a drift behind maneuver (case B) with respect to the same virtual point, see Fig. 2(b). Note that the radius r_1 of the periapse in the case A (or the apoapse in the case B) is given by the equation

$$\frac{r_1}{r_0} = 2\,(1-y)^{2/3} - 1 \tag{4}$$

From the previous results the performance of a phasing maneuver turns out to be a suitable trade-off among conflicting requirements such as the mission velocity variation ΔV, the total flight time Δt, and the maximum (or minimum) admissible distance r_1 from the primary's center-of-mass O.

2.2 Application to a concrete example

The variation of $\Delta V/v_0$ with $|y|$, see Eq. (2), is drawn in Fig. 3. This figure clearly shows that, for suitable values of y, the total velocity variation of the maneuver corresponds to a significant fraction of the parking orbit's circular velocity v_0. In that case the corresponding propellant consumption would imply a marked variation of the spacecraft mass, taking into account the typical values of the specific impulse for a chemical (i.e. a high thrust) propulsion system. For illustrative purposes assume a heliocentric ($\mu = \mu_\odot = 132\,712\,439\,935\,\mathrm{km^3/s^2}$) circular orbit of radius $r_0 = 1\,\mathrm{au}$ and $v_0 \simeq 29.784\,\mathrm{km/s}$, a single-revolution phasing orbit (i.e. $n = 1$) and a phasing angle $\Delta\theta = 30\,\mathrm{deg}$. From Eq. (1) the dimensionless parameter is $y = 1/12$, which implies a required velocity variation $\Delta V \simeq 0.06\,v_0 \simeq 1.8\,\mathrm{km/s}$ for a drift ahead maneuver (case A), see also Eq.(2). In that case, using the rocket equation and assuming a specific impulse of 400 s, the required propellant mass ratio would be about 37%. Note that the flight time in this mission scenario is $\Delta t \simeq 335$ days, and the perihelion radius is $r_1 \simeq 0.887$ au, see Eqs. (3)-(4).

3 The E-sail option

Consider the dynamics of a spacecraft that initially covers a heliocentric circular orbit with radius r_0, and assume that the spacecraft is equipped with a primary propulsion system constituted by an E-sail. The in-orbit repositioning problem can be conveniently studied using a polar heliocentric reference frame $\mathcal{T}(O; r, \theta)$, in which the angular variable θ is measured counterclockwise starting from the Sun-spacecraft direction at the beginning of the phasing maneuver (time $t = t_0 \triangleq 0$) and the radial direction coincides, to a first order approximation, with the propagation direction of the solar wind.

3.1 Mathematical model

The spacecraft dynamics in the polar heliocentric reference frame is described by the following set of differential equations, see Fig. 4 .

$$\dot{r} = u \tag{5}$$

$$\dot{\theta} = \frac{v}{r} \tag{6}$$

$$\dot{u} = -\frac{\mu_\odot}{r^2} + \frac{v^2}{r} + \tau\, a_0 \left(\frac{r_0}{r}\right) \cos\alpha \tag{7}$$

$$\dot{v} = -\frac{u\, v}{r} + \tau\, a_0 \left(\frac{r_0}{r}\right) \sin\alpha \tag{8}$$

where u and v are, respectively, the radial and circumferential component of the spacecraft velocity, $\tau = \{0,\, 1\}$ is the switching parameter, which allows the propulsive acceleration modulus to be set equal to zero to account for the presence of coasting arcs during the orbit transfer, and a_0 is the maximum propulsive acceleration on the circular orbit of radius r_0. In particular, the variation law of the propulsive acceleration with the distance from the Sun is in accordance with the recent plasma dynamic simulations by Janhunen [13].

Note that a_0 coincides with the spacecraft characteristic acceleration a_c when the radius of the parking orbit is one astronomical unit. More precisely, the relation between a_0 and a_c is

$$a_c = a_0 \left(\frac{r_0}{r_\oplus} \right) \tag{9}$$

where $r_\oplus \triangleq 1\,\text{au}$. Finally, $\alpha \in [-\alpha_{\max}, \alpha_{\max}]$ in Eqs. (7)-(8) is the cone angle, i.e. the angle between the Sun-spacecraft line and the thrust direction. The modulus of the cone angle is constrained to not exceed an upper bound, which in this paper is assumed to be $\alpha_{\max} \triangleq 30\,\text{deg}$.

A set of canonical units is now introduced to reduce the numerical sensitivity in the integration of the differential equations and to make the simulation results independent of the radius of the initial parking orbit. The canonical values of distance (DU) and time (TU) are defined as

$$\text{DU} \triangleq r_0 \qquad , \qquad \text{TU} \triangleq \sqrt{\frac{r_0^3}{\mu_\odot}} \tag{10}$$

Note that a_0, when expressed in canonical units, coincides with the ratio of the propulsive acceleration modulus to the gravitational acceleration modulus along the parking orbit (the latter being $\mu_\odot / r_0^2$). Recalling that the parking orbit is circular, the four state variables at time t_0 are given by

$$r(t_0) = 1\,\text{DU} \quad , \quad \theta(t_0) = 0 \quad , \quad u(t_0) = 0\,\text{DU/TU} \quad , \quad v(t_0) = 1\,\text{DU/TU} \tag{11}$$

while the Sun's gravitational parameter is unitary, that is, $\mu_\odot = 1\,\mathrm{DU}^3/\mathrm{TU}^2$.

For a given value of a_0, the problem is to minimize the time interval $\Delta t = t_f$ (where t_f is the final time) required to accomplish a phasing maneuver of a prescribed angle $\Delta\theta$. This amounts to maximizing the scalar performance index

$$J \triangleq -\Delta t = -t_f \tag{12}$$

where the boundary conditions to be met at the final time are

$$r(t_f) = 1\,\mathrm{DU}\ ,\ \theta(t_f) = t_f\sqrt{\frac{\mu_\odot}{r_0^3}} + \Delta\theta\ ,\ u(t_f) = 0\,\mathrm{DU/TU}\ ,\ v(t_f) = 1\,\mathrm{DU/TU} \tag{13}$$

Using an indirect approach, introduce the Hamiltonian function $\mathcal{H}$, which, recalling the equations of motion (5)–(8), is given by

$$\mathcal{H} \triangleq \lambda_r\, u + \frac{\lambda_\theta\, v}{r} + \lambda_u \left[-\frac{\mu_\odot}{r^2} + \frac{v^2}{r} + \tau\, a_0 \left(\frac{r_0}{r}\right) \cos\alpha\right] + \lambda_v \left[-\frac{u\, v}{r} + \tau\, a_0 \left(\frac{r_0}{r}\right) \cos\alpha\right] \tag{14}$$

where λ_r, λ_θ, λ_u and λ_v are the adjoint variables associated with r, θ, u and v, respectively. The time derivative of the generic adjoint variable is obtained from the Euler-Lagrange equations:

$$\dot\lambda_r \triangleq -\frac{\partial\mathcal{H}}{\partial r} = \frac{\lambda_\theta\, v}{r^2} - \lambda_u \left[-\frac{v^2}{r^2} + \frac{2\,\mu_\odot}{r^3} - \tau\, a_0 \left(\frac{r_0}{r^2}\right) \cos\alpha\right] - \lambda_v \left[\frac{u\, v}{r^2} - \tau\, a_0 \left(\frac{r_0}{r^2}\right) \sin\alpha\right] \tag{15}$$

$$\dot\lambda_\theta \triangleq -\frac{\partial\mathcal{H}}{\partial\theta} = 0 \tag{16}$$

$$\dot\lambda_u \triangleq -\frac{\partial\mathcal{H}}{\partial u} = -\lambda_r + \frac{\lambda_v\, v}{r} \tag{17}$$

$$\dot\lambda_v \triangleq -\frac{\partial\mathcal{H}}{\partial v} = -\frac{\lambda_\theta + 2\,\lambda_u\, v - \lambda_v\, u}{r} \tag{18}$$

As a consequence of Eq. (16), the adjoint variable λ_θ turns out to be a constant of motion.

The two-point boundary value problem (TPBVP) associated to the minimum time problem is therefore constituted by the four equations of motion (5)–(8) and the four Euler-Lagrange equations (15)–(18). The corresponding boundary conditions are the four initial conditions (11) and the four final conditions (13) to be calculated at the unknown final time t_f. The latter is found by enforcing the transversality condition that, taking into account Eq. (12) and the second of Eqs. (13), is written as

$$\mathcal{H}(t_f) = 1 + \lambda_\theta \sqrt{\frac{\mu_\odot}{r_0^3}} \tag{19}$$

The two control variables (i.e. the switching parameter τ and the cone angle α) are obtained using the Pontryagin's maximum principle, by maximizing, at any time, the portion $\mathcal{H}'$ of the Hamiltonian that explicitly depends on the control variables, viz.

$$\mathcal{H}' \triangleq \tau \, (\lambda_u \, \cos\alpha + \lambda_v \, \sin\alpha) \tag{20}$$

Taking into account the constraint on the maximum value of the cone angle α, the optimal control law is given by

$$\alpha = \begin{cases} \operatorname{sign}(\lambda_v) \, \arccos\left[\dfrac{\lambda_u}{\sqrt{\lambda_u^2 + \lambda_v^2}}\right] & \text{if} \quad \arccos\left[\dfrac{\lambda_u}{\sqrt{\lambda_u^2 + \lambda_v^2}}\right] \leq \alpha_{\max} \\ \operatorname{sign}(\lambda_v) \, \alpha_{\max} & \text{if} \quad \arccos\left[\dfrac{\lambda_u}{\sqrt{\lambda_u^2 + \lambda_v^2}}\right] > \alpha_{\max} \end{cases} \tag{21}$$

and

$$\tau = \begin{cases} 1 & \text{if} \quad (\lambda_u \, \cos\alpha + \lambda_v \, \sin\alpha) \geq 0 \\ 0 & \text{if} \quad (\lambda_u \, \cos\alpha + \lambda_v \, \sin\alpha) < 0 \end{cases} \tag{22}$$

where $\operatorname{sign}(\square)$ is the signum function.

3.2 Numerical Resolution of the problem

For a given pair of mission parameters $\{a_0, \Delta\theta\}$, the minimum flight time Δt and the corresponding time histories of the state variables are found by numerically solving the TPBVP associated to the optimization problem. The approach used in the solution is described in Ref. [7], while the differential equations have been integrated in double precision using a variable order Adams-Bashforth-Moulton solver scheme [14,15] with absolute and relative errors of 10^{-12}.

4 Application to a mission scenario

The optimal performance of a phasing maneuver along a heliocentric circular orbit of radius r_0 has been studied using the approach described in the previous section. The minimum (optimal) flight time Δt has been numerically calculated as a function of the maximum propulsive acceleration and of the phasing angle, which are varied in the ranges $a_0 \in [0.02, 0.5]\,\mathrm{DU/TU^2}$ and $\Delta\theta \in [-60, 60]\,\mathrm{deg}$, respectively. Recall, with the adopted convention, that $\Delta\theta > 0$ implies a drift ahead maneuver (case A), while $\Delta\theta < 0$ represents a drift behind maneuver (case B). Also note that $a_0 = 0.5\,\mathrm{DU/TU^2}$ corresponds to a maximum propulsive acceleration equal to one half the local solar gravitational acceleration at the beginning (and at the end) of the transfer. In this sense, a value of a_0 greater than 0.5 is well beyond the current potential performance of an E-sail-based propulsion system for a phasing maneuver involving the heliocentric Earth's orbit (i.e. $r_0 = r_\oplus$).

The simulation results are summarized in Fig. 5(a) for case A, and in Fig. 5(b) for case B. These two figures represent the contour lines of the surface $\Delta t =$

$\Delta t\,(a_0,\,\Delta\theta)$. In both cases, for a given $\Delta\theta$, there is a marked increase in the required flight time when a_0 is decreased. Also, for a given pair $(a_0,\,|\Delta\theta|)$, the drift behind maneuver takes advantage of the spacecraft motion along the circular parking orbit and, as such, always needs a flight time smaller than that required in a drift ahead maneuver. For example, assuming a propulsive acceleration equal to a tenth the local gravitational attraction (i.e. $a_0 = 0.1\,\mathrm{DU}/\mathrm{TU}^2$), a drift ahead maneuver of 30 deg requires a flight time about 1.2 times the orbital period T_0 of the parking orbit. The same spacecraft could complete a drift behind maneuver of 30 deg within a flight time of $0.7\,T_0$, with a reduction of over 40% of T_0 when compared to case A. Recall that a two-impulse phasing maneuver of 30 deg requires a velocity variation $\Delta V/v_0$ equal to 6% (or 5%) for a drift ahead (or behind).

4.1 Earth's orbit phasing

The results summarized in Fig. 5 are independent of the radius r_0 of the parking orbit and, therefore, they can be applied to different mission scenarios involving heliocentric circular parking orbits. The most interesting case concerns a phasing maneuver along the Earth's heliocentric orbit. This corresponds to a situation in which the spacecraft escapes from the Earth's gravitational field using a parabolic orbit (relative to the Earth) and, once outside the Earth's sphere of influence, it tracks a nearly circular orbit (with a radius $r_0 = r_\oplus$) around the Sun.

The previous results can be specialized to this noteworthy scenario by simply observing from Eq. (9) that in this case a_0 coincides with the E-sail characteristic acceleration a_c. In particular, the analysis involves different values of the characteristic acceleration, which is assumed to range in the interval $[0.1,\,1]\,\mathrm{mm/s^2}$.

The upper bound of the interval reflects the value that is estimated to be reached by the E-sail technology in a near future. The simulation results have been collected with the aid of contour lines of the function $\Delta t = \Delta t(a_c, \Delta\theta)$ and are shown in Fig. 6. The characteristic acceleration a_c is parameterized with a step variation of $0.1\,\mathrm{mm/s^2}$.

4.2 Reaching triangular Lagrangian points

An interesting conclusion can be deduced by carefully analyzing the previous results. Consider an E-sail with a characteristic acceleration $a_c = 1\,\mathrm{mm/s^2}$ and assume that the phasing angle to be met is $|\Delta\theta| = 60\,\mathrm{deg}$. From Fig. 6(a) the required flight time for a drift ahead maneuver is 450 days, while it reduces to about 286 days for a drift behind maneuver, see Fig. 6(b). These flight times are nearly coincident with those obtained in Ref. [7] for an optimal transfer between the two classical Lagrange points $L_1 \to L_4$ (445 days), and $L_1 \to L_5$ (287 days) of the Sun-[Earth+Moon] Circular Restricted Three-Body Problem (CRTBP). Note that the simulation results in Ref. [7] were obtained assuming a three-dimensional dynamics and taking into account the gravitational attraction of both the Sun and that of Earth+Moon planetary system. The similarity of the results of this paper with those of Ref. [7] is by no means surprising. As a matter of fact, the Sun and the triangular Lagrangian points (L_4 and L_5) are at the vertices of an equilateral triangle with a side equal to 1 au, while L_1 is along the Sun-Earth line at a distance of about 0.99 au from the star, see Fig. 7.

Therefore, neglecting the Earth+Moon gravitational attraction (thus reducing the problem to a two-body motion involving the Sun and the spacecraft only) and approximating the L_1 point location with a distance equal to $r_\oplus$ from the

Sun, the transfer $L_1 \to L_4$ is nearly coincident with a drift ahead maneuver of an angle $\Delta\theta = 60\,\mathrm{deg}$, while the transfer $L_1 \to L_5$ is close to a drift behind maneuver of an angle $\Delta\theta = -60\,\mathrm{deg}$. More generally, using the results shown in Fig. 6 when $|\Delta\theta| = 60\,\mathrm{deg}$, it is possible to have a first order estimate of the minimum flight times required to transfer a spacecraft from L_1 to L_4 or from L_1 to L_5 as a function of the magnitude of the characteristic acceleration. These data, reported in Fig. 8, extend the results discussed in Ref. [7] that were confined to a single value of spacecraft characteristic acceleration only, i.e. $a_c = 1\,\mathrm{mm/s^2}$.

In particular, Fig. 8 points out the marked nonlinear relation between minimum flight time and spacecraft characteristic acceleration. For example, a characteristic acceleration reduction of a factor two, from $1\,\mathrm{mm/s^2}$ to $0.5\,\mathrm{mm/s^2}$ (possibly due to a doubling of the spacecraft launch mass) would imply a flight time increase of 25% in a transfer to L_5 (corresponding to a total flight time of about 353 days), but a time increase of 12% only in a transfer to L_4 (with a total flight time of 504 days). Note that the flight time sensitivity to a variation of the characteristic acceleration tends to decrease by increasing the value of a_c, that is, by improving the performance of the propulsion system.

The shape of the transfer trajectory, for a fixed phasing angle $\Delta\theta$, is strongly dependent on the value of the characteristic acceleration. A significant example of the different trajectories that can be obtained is illustrated in Fig. 9, which shows the results when $a_c = \{0.1,\, 1\}\,\mathrm{mm/s^2}$, for the two cases of either drift ahead maneuver with $\Delta\theta = 60\,\mathrm{deg}$ (see Fig. 9(a)), or a drift behind maneuver with $\Delta\theta = -60\,\mathrm{deg}$ (Fig. 9(b)). Note that the trajectories of Fig. 9 are drawn in a reference frame that rotates around the Sun with an angular velocity equal to that of the Earth's circular orbit. In particular, the E-sail trajectories reveal the existence of coasting phases during the transfer, whose number and length depend both on the phasing type (ahead or behind maneuver) and on the characteristic acceleration value. Note that in a drift ahead maneuver the trajectory is inside the Earth's circular orbit, while in a drift behind maneuver the spacecraft distance from the Sun is always greater than $r_\oplus$, and the shape of the transfer trajectory for the case $a_c = 1\,\mathrm{mm/s^2}$ is very close to that found in Ref. [7].

4.3 Choosing between drift ahead and drift behind in a mission design

The simulation results have another interesting application. Assume that a given point along the circular parking orbit, characterized by an angular distance $\Delta\overline{\theta} \in (0,\,360)$ deg from the initial position, is to be reached either with a drift ahead maneuver (therefore $\Delta\theta \equiv \Delta\overline{\theta}$), or with a drift behind maneuver (that is, $\Delta\theta = 360 - \Delta\overline{\theta}$). It has been shown that, the characteristic acceleration being the same, the performance is remarkably different for the two phasing maneuvers. It is therefore possible to look for the value $\Delta\overline{\theta}$ below which a drift ahead maneuver is better (i.e., it requires smaller flight times) than a drift behind maneuver. An example is shown in Fig. 10, which illustrates the minimum flight time as a function of $\Delta\overline{\theta}$ for a characteristic acceleration $a_c = 1\,\mathrm{mm/s^2}$.

Figure 10 shows that when $\Delta\overline{\theta} > 160\,\mathrm{deg}$, the final position along the circular orbit being the same, a drift behind maneuver guarantees a flight time less than that required by a drift ahead maneuver. This is a counterintuitive and useful result, as it gives, with a reduced computational time, a precise information on the best strategy to be used in this mission scenario.

5 Conclusions

The conducted analysis and the numerical simulations show that the Electric Solar Wind Sail is a potentially interesting option for an in-orbit repositioning problem of a spacecraft placed along a circular heliocentric orbit. The intrinsic capability of this propulsion system to produce a propulsive thrust without the use of propellant, guarantees the possibility of overcoming the limitations of conventional propulsion systems related to the large velocity variations they require to perform the maneuver. The flight times required to complete the transfer are comparable to that necessary for a two-impulse maneuver, using a propulsion system with medium-low performance.

The proposed method gives interesting information involving a transfer mission to the triangular Lagrange's points of the Sun-[Earth+Moon] system, with a reduced amount of simulation time. The parametric approach allows the sensitivity to mission performance to be estimated as a function of the propulsion system performance (expressed in terms of characteristic acceleration modulus). The obtained results are a good starting point for a more refined analysis of a transfer toward the triangular Lagrange's points, which could take into account, for example, the spatial-temporal irregularity of the solar wind.

References

[1] V. A. Chobotov (Ed.), Orbital Mechanics, 3rd Edition, AIAA Education Series, American Institute of Aeronautics and Astronautics, New York, 2002, Ch. 7, pp. 152–155, ISBN: 1-56347-537-5.

[2] H. D. Curtis, Orbital Mechanics for Engineering Students, 3rd Edition,

Butterworth-Heinemann, 225 Wyman Street, Waltham, 02451, USA, 2014, Ch. 6, pp. 312–317, ISBN: 978-0-08-097747-8.

[3] C. R. McInnes, Azimuthal repositioning of payloads in heliocentric orbit using solar sails, Journal of Guidance, Control, and Dynamics 26 (4) (2003) 662–664, doi: 10.2514/2.5098.

[4] G. Mengali, A. A. Quarta, In-orbit repositioning of multiple solar sail spacecraft, Aerospace Science and Technology 12 (7) (2008) 506–514, doi: 10.1016/j.ast.2007.12.003.

[5] A. A. Quarta, G. Mengali, Optimal solar sail phasing trajectories for circular orbit, Journal of Guidance, Control, and Dynamics 36 (6) (2013) 1821–1824, doi: 10.2514/1.59372.

[6] P. Janhunen, P. K. Toivanen, J. Polkko, S. Merikallio, P. Salminen, E. Haeggström, H. Seppänen, R. Kurppa, J. Ukkonen, S. Kiprich, G. Thornell, H. Kratz, L. Richter, O. Krömer, R. Rosta, M. Noorma, J. Envall, S. Lätt, G. Mengali, A. A. Quarta, H. Koivisto, O. Tarvainen, T. Kalvas, J. Kauppinen, A. Nuottajärvi, A. Obraztsov, Electric solar wind sail: Toward test missions, Review of Scientific Instruments 81 (11) (2010) 111301–1–11301–11, doi: 10.1063/1.3514548.

[7] A. A. Quarta, G. Aliasi, G. Mengali, Electric solar wind sail optimal transit in the circular restricted three body problem, Acta Astronautica 116 (2015) 43-49, doi:10.1016/j.actaastro.2015.06.017.

[8] M. Connors, P. Wiegert, C. Veillet, Earth's trojan asteroid, Nature 475 (2011) 481–483, doi: 10.1038/nature10233.

[9] W. Miyake, Y. Saito, H. Hayakawa, A. Matsuoka, On the correlation of the solar wind observed at the l5 point and at the earth, Advances in Space Research 36 (12) (2005) 2328–2332, doi: 10.1016/j.asr.2004.06.019.

[10] K. D. C. Simunac, L. M. Kistler, A. B. Galvin, M. A. Popecki, C. J. Farrugia, In situ observations from stereo/plastic: a test for L5 space weather monitors, Annales Geophysicae 27 (2009) 3805–3809, doi: 10.5194/angeo-27-3805-2009, 2009.

[11] D. F. Webb, et al., Using STEREO-B as an L5 space weather pathfinder mission, Space Research Today 178 (2010) 10–16, doi: 10.1016/j.srt.2010.07.004.

[12] N. Gopalswamy, et al., Earth-affecting solar causes observatory (EASCO): A potential international living with a star mission from Sun-Earth L5, Journal of Atmospheric and Solar-Terrestrial Physics 73 (5-6) (2011) 658–663, doi: 10.1016/j.jastp.2011.01.013.

[13] P. Janhunen, The electric solar wind sail status report, in: European Planetary Science Congress 2010, Vol. 5, Rome, Italy, 2010, paper EPSC 2010-297.

[14] L. F. Shampine, M. K. Gordon, Computer Solution of Ordinary Differential Equations: The Initial Value Problem, W. H. Freeman, San Francisco, 1975, Ch. 10.

[15] L. F. Shampine, M. W. Reichelt, The MATLAB ODE suite, SIAM Journal on Scientific Computing 18 (1) (1997) 1–22 .

List of Figures

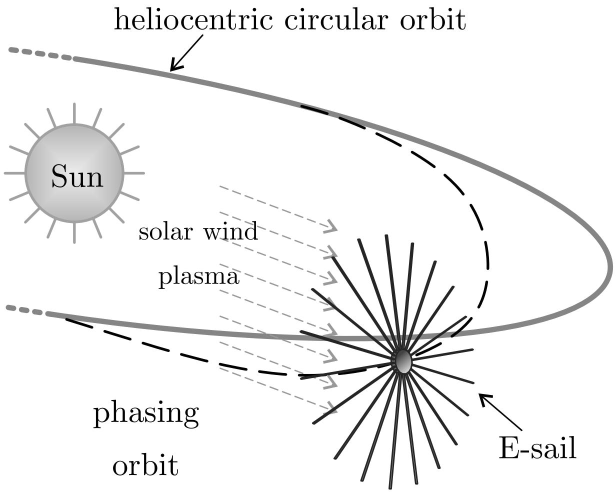

Figure 1. In-orbit repositioning of a E-sail-based spacecraft: conceptual scheme. We assume a radial direction of the solar wind plasma propagation.

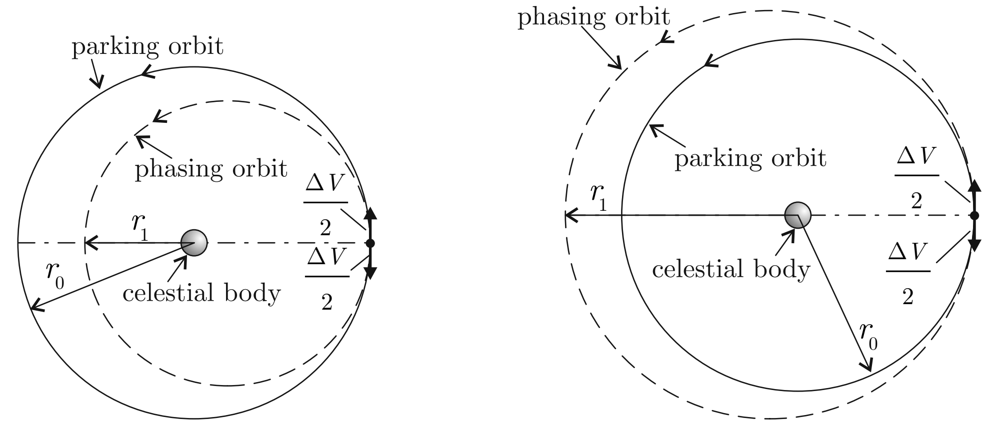

(a) Drift ahead maneuver (case A).

(b) Drift behind maneuver (case B).

Figure 2. In-orbit repositioning with a two-impulse, tangential, phasing orbit. The parking orbit is circular and the spacecraft covers an inner (outer) phasing orbit when a drift ahead (behind) is considered.

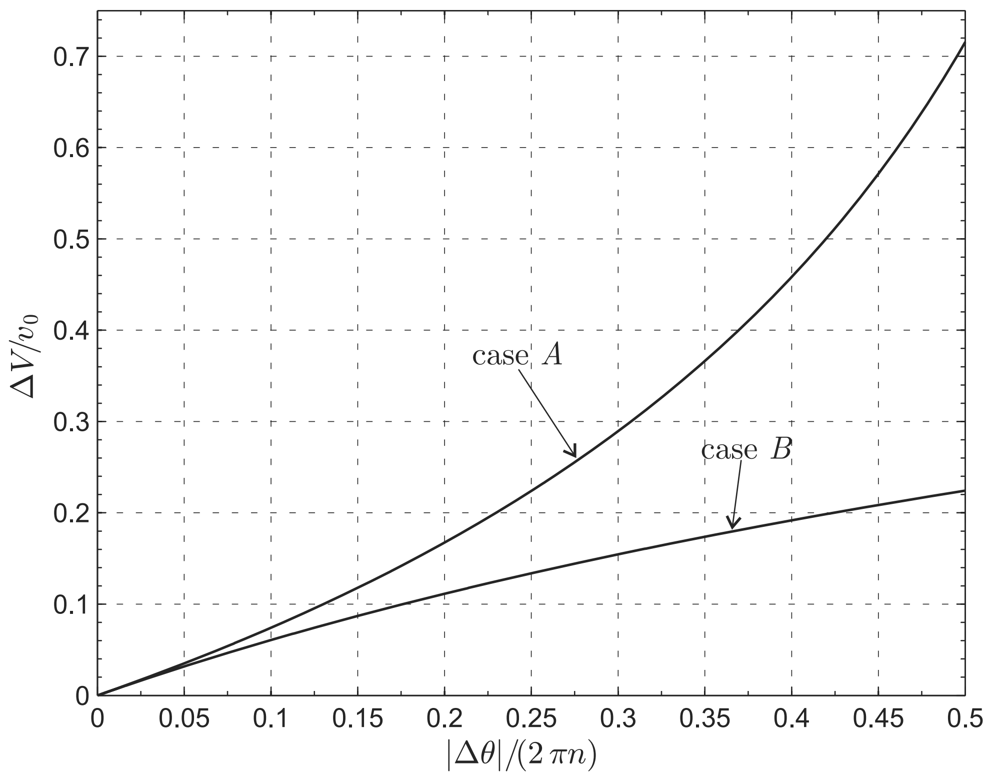

Figure 3. Dimensionless velocity variation $\Delta V/v_0$, where v_0 is the parking circular orbit speed, as a function of the phasing angle in a two-impulse mission case, see Eq. (2). Case A (or B) refers to a drift ahead (or behind).

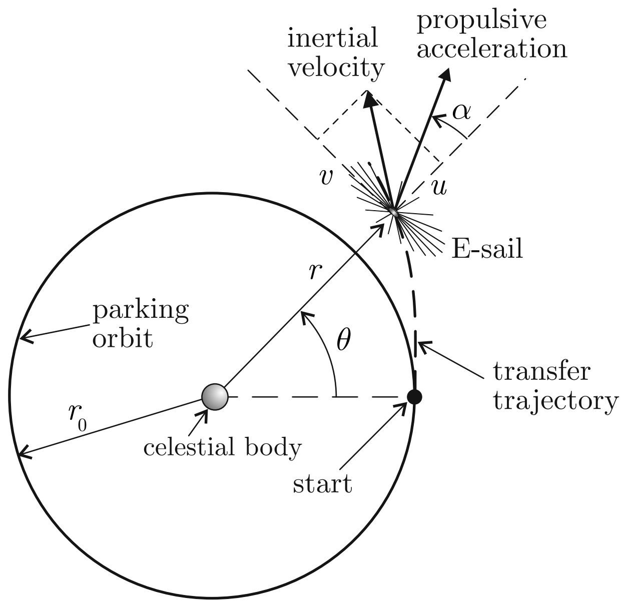

Figure 4. Reference frame.

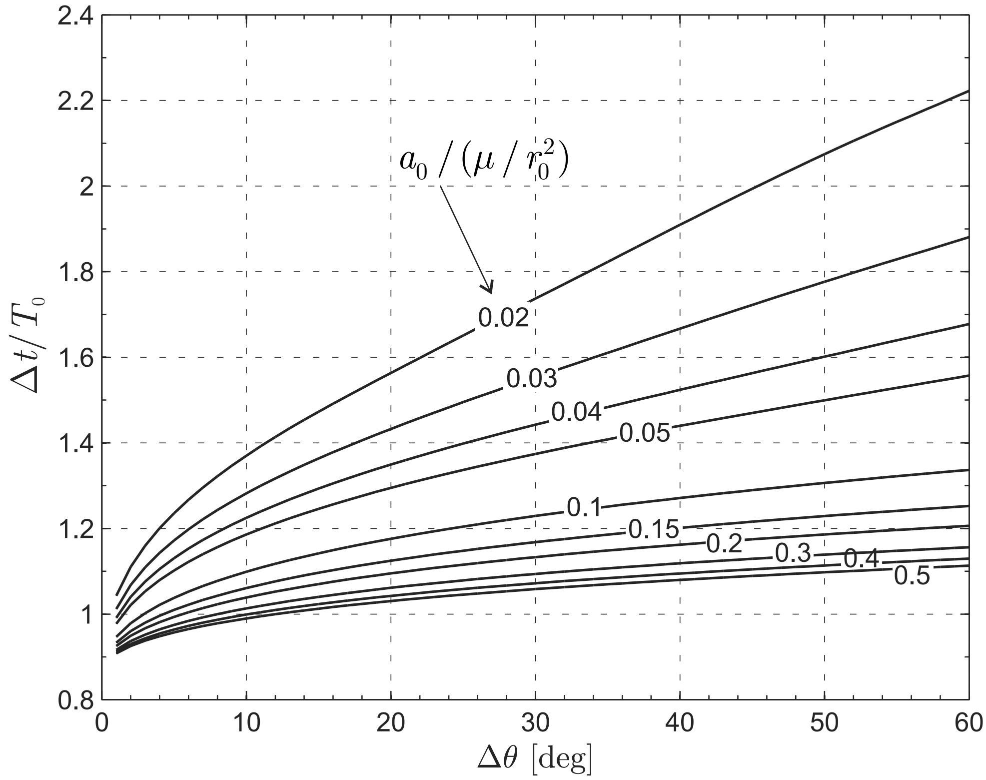

(a) Drift ahead maneuver (case A).

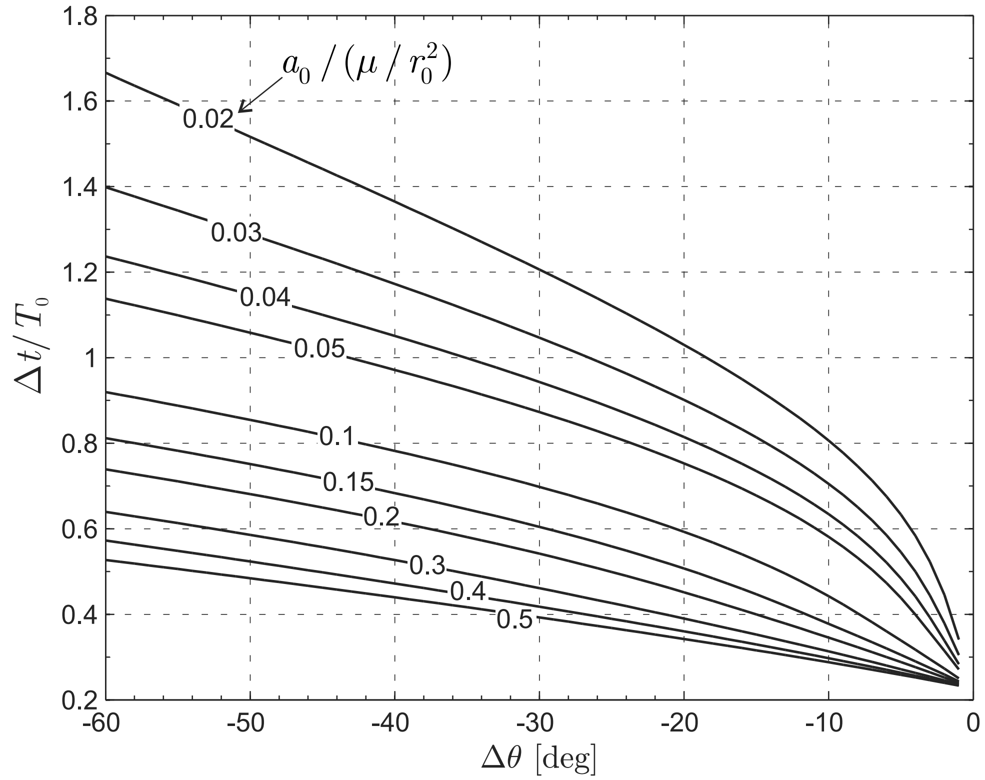

(b) Drift behind maneuver (case B).

Figure 5. Dimensionless minimum flight time $\Delta t/T_0$, where T_0 is the parking orbit period, as a function of the maximum propulsive acceleration a_0 and phasing angle $\Delta\theta$.

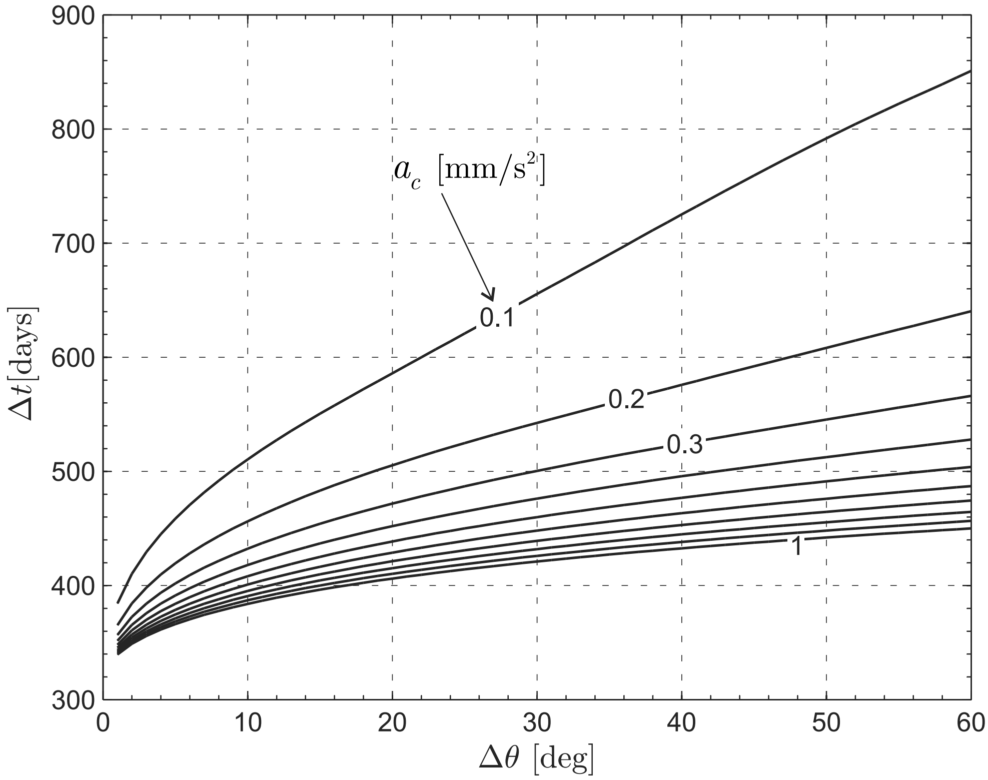

(a) Drift ahead maneuver.

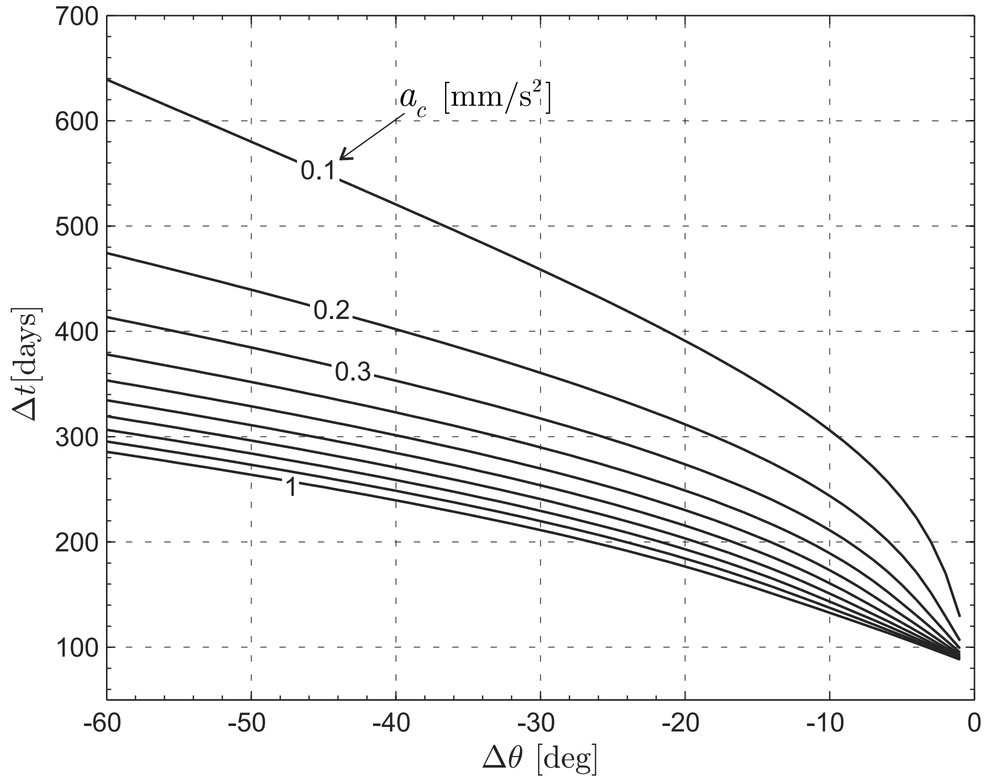

(b) Drift behind maneuver.

Figure 6. Earth's orbit phasing mission scenario: minimum flight time as a function of the characteristic acceleration a_c and phasing angle $\Delta\theta$.

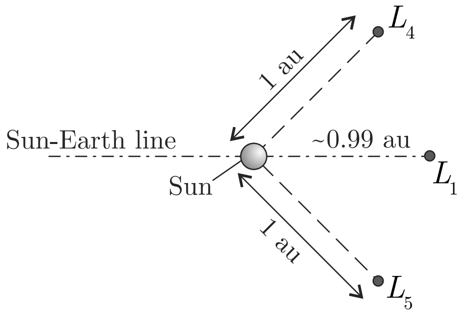

Figure 7. Approximate positions of the classical Lagrangian points L_1, L_4 and L_5 in the Sun-[Earth+Moon] planetary system.

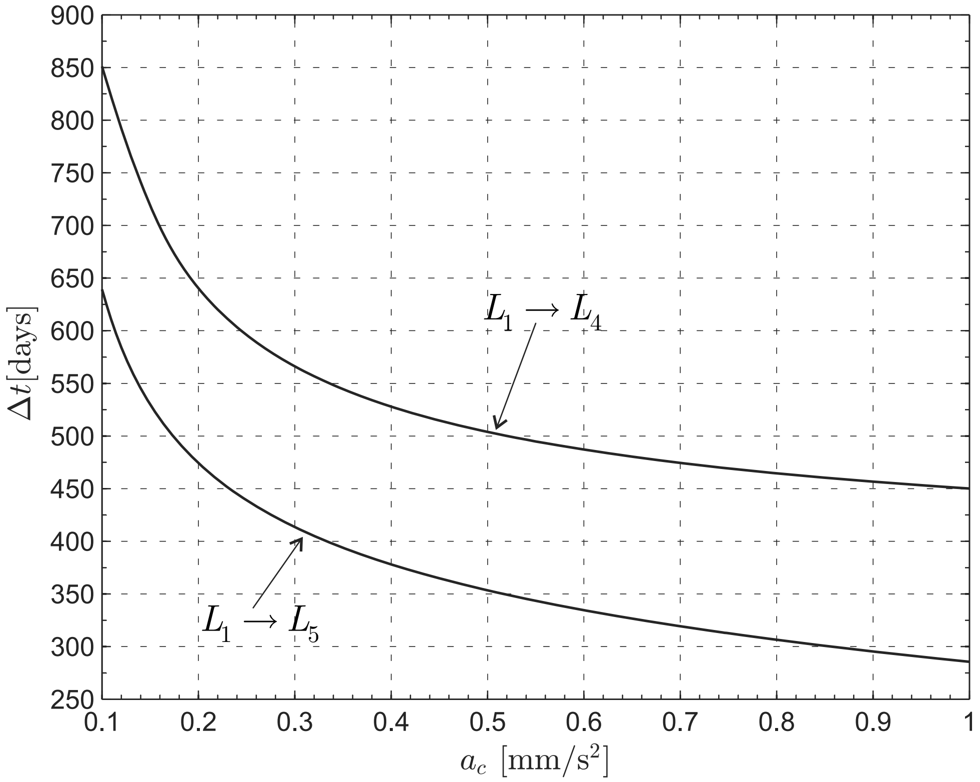

Figure 8. Approximate minimum flight time between Lagrangian points L_1 and L_4 (or L_5) of the Sun-[Earth+Moon] planetary system, as a function of the characteristic acceleration a_c.

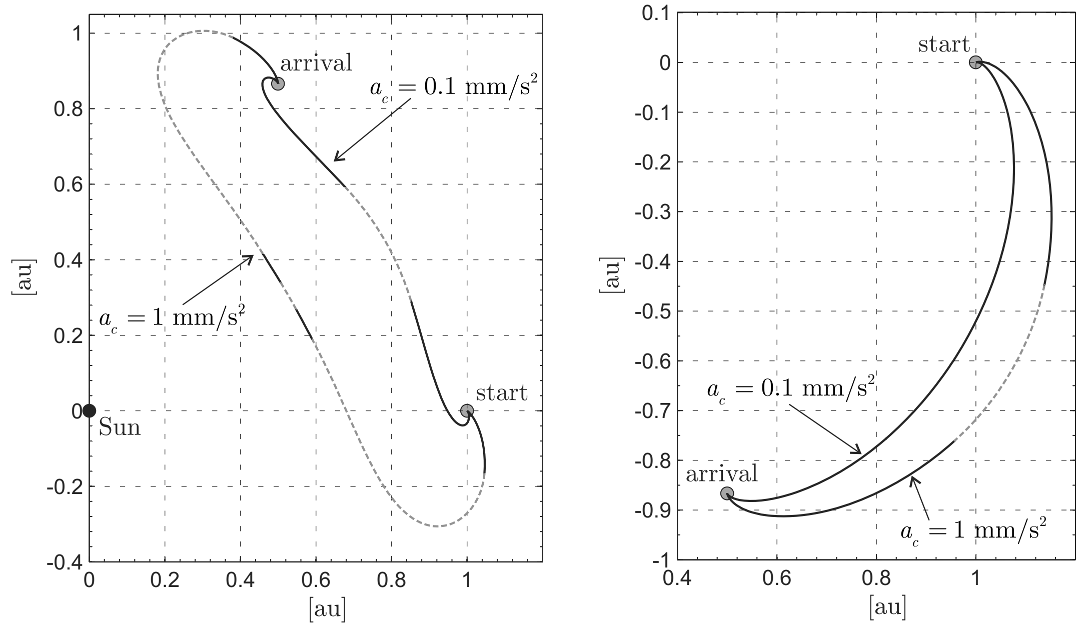

(a) Drift ahead maneuver $\Delta\theta = 60\,\text{deg}$.

(b) Drift behind maneuver $\Delta\theta = -60\,\text{deg}$.

Figure 9. Optimal phasing transfer trajectories when $a_c = \{0.1,\, 1\}$ mm/s^2 (solid line: thruster on; dashed line: thruster off).

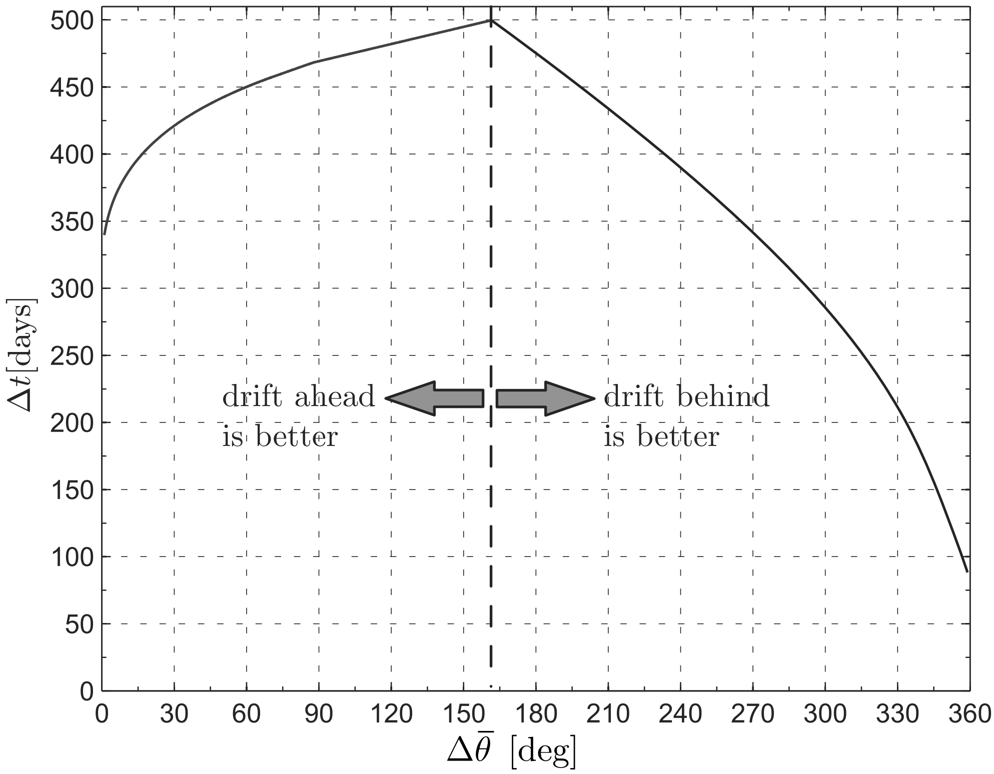

Figure 10. Earth's orbit phasing mission scenario: minimum flight time as a function of the phasing angle $\Delta\theta$, for a canonical value of the characteristic acceleration ($a_c = 1$ mm/s^2).